

# We are IntechOpen, the world's leading publisher of Open Access books Built by scientists, for scientists

5,400

Open access books available

133,000

International authors and editors

165M

Downloads

Our authors are among the

154

Countries delivered to

TOP 1%

most cited scientists

12.2%

Contributors from top 500 universities



WEB OF SCIENCE™

Selection of our books indexed in the Book Citation Index  
in Web of Science™ Core Collection (BKCI)

Interested in publishing with us?  
Contact [book.department@intechopen.com](mailto:book.department@intechopen.com)

Numbers displayed above are based on latest data collected.  
For more information visit [www.intechopen.com](http://www.intechopen.com)



# Application of Stopped-Flow and Time-Resolved X-Ray Absorption Spectroscopy to the Study of Metalloproteins Molecular Mechanisms

Moran Grossman and Irit Sagi

*Departments of Structural Biology and Biological Regulation,  
The Weizmann Institute of Science, Rehovot  
Israel*

## 1. Introduction

### 1.1 Metalloproteins as mediators of life processes

Revealing detailed molecular mechanisms associated with metalloproteins is highly desired for the advancement of both basic and clinical research. Metalloproteins represent one of the most diverse classes of proteins, containing intrinsic metal ions which provide catalytic, regulatory, or structural roles critical to protein function. The metal ion is usually coordinated by nitrogen, oxygen, or sulfur atoms belonging to amino acids in a polypeptide chain and/or in a macrocyclic ligand incorporated into the protein. The presence of a metal ion rich in electrons allows metalloproteins to perform functions such as redox reactions, phosphorylation, electron transfer, and acid-base catalytic reactions that cannot easily be performed by the limited set of functional groups found in amino acids. Approximately one-third of all proteins possess a bound metal<sup>1</sup>, and almost half of all enzymes require the presence of a metal atom to function<sup>2</sup>. The most abundant metal ions *in vivo* are Mg and Zn, while Fe, Ca, Co, Mn, and Ni are also frequently observed. Metalloproteins play important roles in key biological processes such as photosynthesis, signaling, metabolism, proliferation, and immune response<sup>3-5</sup>. For instance, the principal oxygen carrier protein in human, hemoglobin, uses iron (II) ions coordinated to porphyrin rings to bind the dioxygen molecules; calmodulin is a calcium-binding protein mediating a large variety of signal transduction processes in response to calcium binding; cytochromes mediate electron transport and facilitate a variety of redox reactions using iron, which interconverts between Fe<sup>2+</sup> (reduced) and Fe<sup>3+</sup> (oxidized) states; and many proteolytic enzymes contain zinc ions in their active sites that is highly crucial for peptide bond hydrolysis reaction.

### 1.2 Metalloenzymes architecture and function

Among metalloproteins there are many families of enzymes that utilize metal ions for catalytic activity (Figure 1). The metal ion is usually located at the active site of the enzyme, creating a highly reactive microenvironment, which is often hard to mimic by *in-vitro* synthesis. Zinc, for instance, was found to be an integral component of more than 300 biological catalysts, and it is functionally essential for enzymes belonging to the main biochemical categories: oxidoreductase, transferase, hydrolases, lyases, isomerases and ligases<sup>4</sup>.

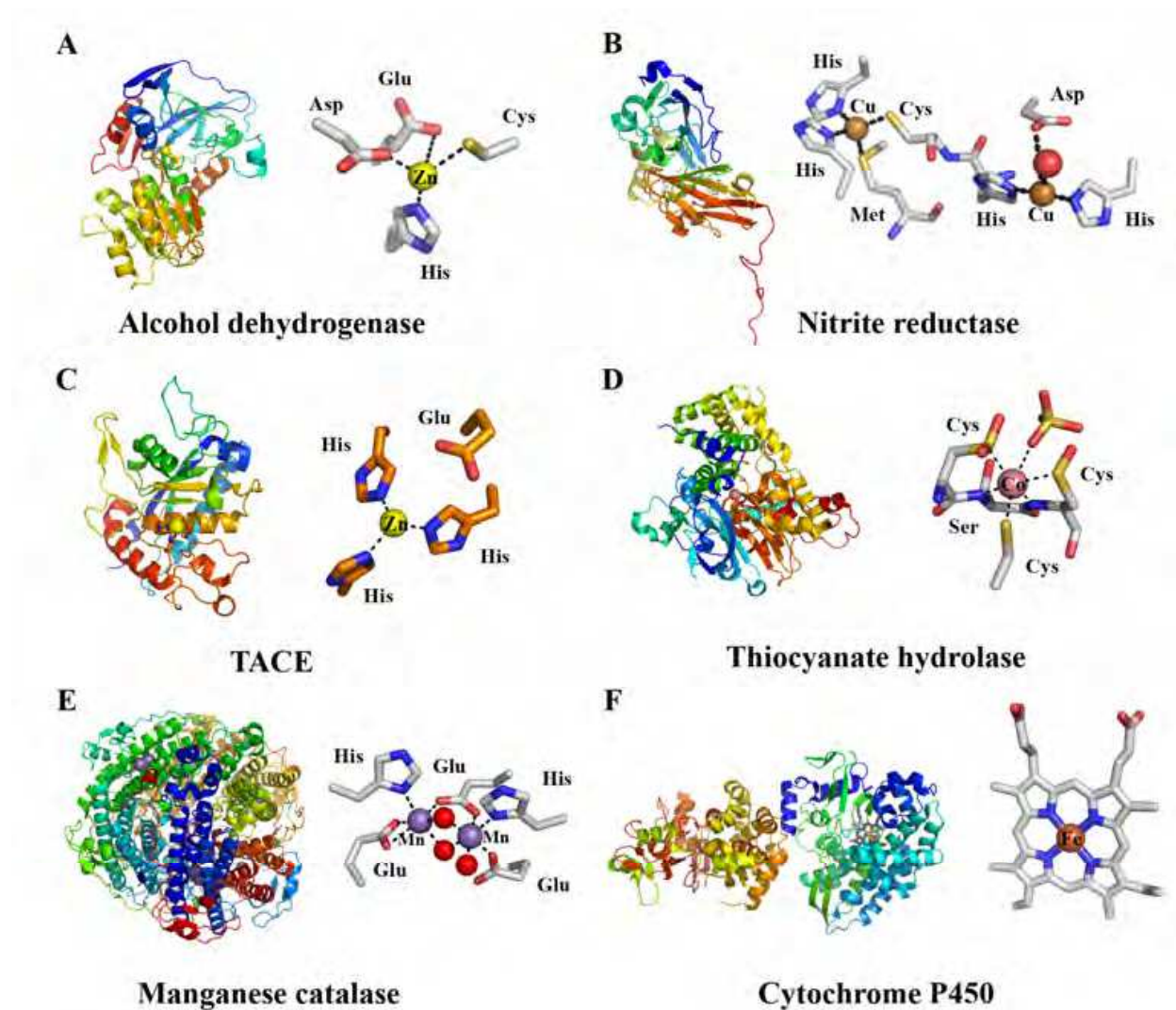


Fig. 1. **Metalloenzymes play key roles in biology.** A) Crystal structure of alcohol dehydrogenase (ADH) from *Thermoanaerobacter brockii* (PDB ID: 1YKF)<sup>11</sup>. ADH catalyzes the reversible oxidation of secondary alcohols to their corresponding ketones using NADP<sup>+</sup>. The catalytic zinc ion is tetrahedrally coordinated by cysteine, histidine, aspartate, and glutamate residues. B) Crystal structure of nitrite reductase from *alcaligenes xylooxidans* (PDB ID: 1OE1)<sup>12</sup>. Nitrite reductase is a key enzyme in denitrification catalyzing the reduction of nitrite (NO<sub>2</sub><sup>-</sup>) to nitric oxide (NO). Two copper centers are involved in the electron transfer. C) Crystal structure of TNF $\alpha$ -converting enzyme (TACE) (PDB ID: 2OI0)<sup>13</sup>. TACE is the main shedding catalysis in the release of tumor necrosis factor- $\alpha$  (TNF $\alpha$ ) from its pro domain. D) Crystal structure of thiocyanate hydrolase from *Thiobacillus thioparus* (PDB ID: 2DD5)<sup>14</sup>. Thiocyanate hydrolase is a cobalt (III)-containing enzyme that catalyzes the degradation of thiocyanate to carbonyl sulfide and ammonia. E) Crystal structure of manganese catalase from *Lactobacillus plantarum* (PDB ID: 1JKU)<sup>15</sup>. Manganese catalase is an important antioxidant metalloenzyme that catalyzes disproportionation of hydrogen peroxide, forming dioxygen and water. F) Cytochrome P450 from *Sulfolobus solfataricus* (PDB ID: 1IO7)<sup>16</sup> belongs to a family of heme containing enzymes that catalyze the oxidation of organic compounds using dioxygen.

For example, the large family of zinc-dependent matrix metalloproteinases (MMPs) is produced as cell-secreted and membrane-tethered enzymes that degrade extracellular matrix (ECM) proteins. These proteases play key roles in diverse physiological and pathological processes, including embryonic development, wound healing, inflammatory diseases, and cancer<sup>6-9</sup>. Zinc is also found in other important families of enzymes such as carbonic anhydrase, alcohol dehydrogenase and carboxypeptidase. This metal ion is special among first-row transition metals due to its filled orbital configuration ( $d^{10}$ ), providing its unique electronic characteristics, such as the ability to shuffle between four, five and six coordination geometries<sup>10</sup>. This flexible coordination chemistry is utilized by metalloenzymes to alter the reactivity of the metal ion, which appears to be important in the mediation of enzyme catalysis. For example, a substrate can bind to the metal ion during catalysis by substituting a bound ligand, or by binding to an empty coordination site. Alternatively, an inhibitor can bind to metal ion by the same mechanism, preventing the coordination of the substrate and thus interfering with catalysis. Therefore, there is a fundamental as well as a practical interest in quantifying the chemical and structural factors that govern mechanisms of action and contribute to catalytic efficiency in such metalloenzyme systems.

### 1.3 Enzymatic mechanisms

The reactions executed by metalloenzymes often involve a cycle of events that take place at the metal-protein's nearest environment during which several intermediate states, varied in their structure, reactivity and energetics, are formed. Therefore, structural and functional characterization of the active site's geometry and elucidation of the catalytic mechanism underlying this fascinating class of enzymes are of critical importance for assigning molecular mechanisms and for rationalizing the design of drugs. However, the identification and characterization of the short-lived metal-ligand/protein intermediates that evolve during catalysis is highly challenging. This is mainly due to the difficulty in directly investigating the detailed dynamic structural and electronic changes occurring in the active site during catalysis. In addition, several metal ions, such as the zinc ion that resides in the active site of MMPs, are spectroscopically silent and hence cannot be studied using conventional spectroscopic techniques. The majority of protein structures presently solved by X-ray crystallography actually correspond to a static state (or a state average) that poorly represents the ensemble of conformations adopted by a protein in action. Although protein structures provide information about protein folds and local structural arrangements, a single static structure is generally insufficient to enable the elucidation of enzymatic catalytic reaction mechanisms at an atomic level of detail. Typically, the catalytic cycle involves a series of intermediates and transition states that cannot be trapped by static or steady-state structural methods. Furthermore, determining the energies of the various stationary points in the cycle is not trivial from a theoretical or experimental point of view. Remarkably, time-resolved protein crystallography has been used to characterize the structure of intermediates that evolve in the course of enzymatic reactions (reviewed in<sup>17, 18</sup>). However, not all important functional intermediates and structural transitions can be captured in a crystalline form.

X-ray absorption spectroscopy (XAS) is one of the most sensitive method to probe the local environment of a metal ion with high spatial resolution ( $0.1\text{\AA}$ ). XAS was developed in the early 1970s as a method to structurally characterize the atomic environment of metal elements found in mineral, noncrystalline solid or adsorbed phases<sup>19</sup>. Nowadays, XAS is

widely used in various fields including mineralogy, geochemistry, materials science and biology. High-quality XAS spectra can be collected on heterogeneous mixtures of gases, liquids, and/or solids with little or no sample pretreatments, making it ideally suited for many chemical and biological systems. In the field of biology, XAS is widely used in structure-function analysis of metalloproteins, as well as in the study of whole tissue or culture. In spite of the increase use of XAS, it is generally utilized as a technique for studying stable or equilibrium states, and not of intermediates. In recent years, with the advances in X-ray light sources and data analysis procedures, the time dimension was introduced into the field of XAS providing insights into the changes in the local structure of metal sites dictating metalloproteins molecular mechanisms. Here, we will describe the theoretical aspects of XAS as well as the development of stopped-flow and time-resolved XAS and discuss recent studies in which these techniques deciphered important molecular mechanisms driving the function of metalloproteins.

## 2. X-ray absorption spectroscopy (XAS)

### 2.1 Theoretical aspects

XAS measures the absorption of X-rays as a function of their energy. Specifically, the X-ray absorption coefficient is determined from the decay of the X-ray beam as it passes through the sample. The number of X-rays transmitted ( $I_t$ ) through a sample is given by the intensity of X-rays impinging on the sample ( $I_0$ ) decreased exponentially by the thickness of the sample ( $x$ ) and the absorption coefficient of the sample ( $\mu$ ):

$$I_t = I_0 e^{-\mu x} \quad (1)$$

In a typical experimental setup for XAS shown in Figure 2, the X-rays go through an ionization chamber to measure the number of incident X-rays ( $I_0$ ), then through the sample, and then through another ionization chamber to measure the number of transmitted X-rays ( $I_t$ ).

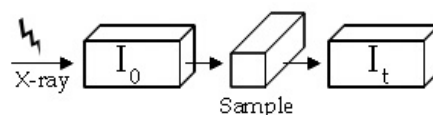


Fig. 2. Schematic drawing of an EXAFS experimental setup.

The X-ray absorption coefficient is determined by rearranging Eq. (1):

$$\mu x = \ln \left( \frac{I_0}{I_t} \right) \quad (2)$$

The X-ray absorption coefficient,  $\mu$ , decreases as the energy increases except for a sudden sharp rise at certain energies called edges. Each such absorption edge is related to a specific atom present in the sample, and it occurs when an incident X-ray photon has just enough energy to cause a transition that excites a particular atomic core-orbital electron to the free or unoccupied continuum level. K-edges, for example, refer to transitions that excite the innermost 1s electron. The spectral region closer to the edge, conventionally within 50 eV of the absorption edge, is called XANES (X-ray absorption near edge structure). This

region is often dominated by strong scattering processes as well as local atomic resonances in the X-ray absorption and is therefore more difficult for quantitative analysis. However, even a qualitative comparison of this region is useful in providing information about the redox state of the metal center and details about the local site symmetry, bond length and orbital occupancy.

Above the edges, there is a series of wiggles or an oscillatory structure that modulates the absorption. In these energies, the created photoelectron also possesses a kinetic energy (KE) which equals to the difference between the incident X-ray energy ( $E$ ) and the electron binding energy of the photoelectron ( $E_0$ ):

$$KE = E - E_0 \quad (3)$$

The photoelectrons can be described as spherical waves propagating outward from the absorber atoms. These photoelectron waves are scattered from the atoms surrounding the absorber. The relative phase of the outgoing photoelectron wave and the scattered wave at the absorbing atom affects the probability for X-ray absorption by the absorber atom. The relative phase is determined by the photoelectron wavelength and the interatomic distances between the absorber and scattering atoms. The outgoing and backscattered photoelectron waves interfere either constructively or destructively, giving rise to the modulations in the X-ray absorption coefficient spectra. Those oscillatory wiggles beyond  $\sim 30\text{eV}$  above the absorption edge contain important high-resolution information about the local atomic structure around the atom that absorbed the X-ray. This region is called extended X-ray absorption fine structure (EXAFS).

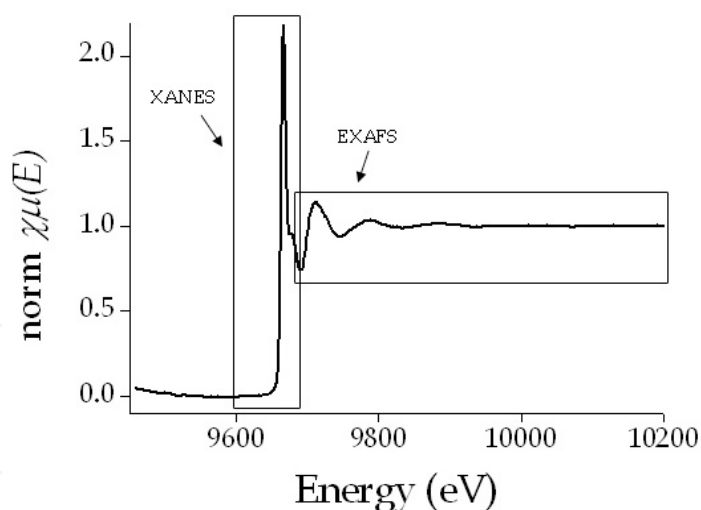


Fig. 3. The X-ray absorption spectrum of  $\text{ZnCl}_2$ . The XANES and EXAFS regions are highlighted.

The EXAFS function  $\chi(E)$  is defined as:

$$\chi(E) = \frac{\mu(E) - \mu_0(E)}{\Delta\mu_0(E)} \quad (4)$$

where  $\mu(E)$  is the measured absorption coefficient,  $\mu_0(E)$  is a smooth background function representing the absorption of an isolated atom, and  $\Delta\mu_0(E)$  is the measured edge step at the

excitation energy,  $E_0$ . Since we can refer to the excited electron as a photoelectron,  $\chi(E)$  is best understood in terms of wave behavior. Therefore, it is common to convert the X-ray absorption to  $k$ , the wave number of the photoelectron, which is defined as:

$$k = \sqrt{\frac{2m(E - E_0)}{\hbar^2}} \quad (5)$$

where  $E_0$  is the absorption edge energy,  $m$  is the electron mass and  $\hbar$  is the Planck constant. The EXAFS region of the spectra provides more detailed structural information and can be quantitatively analyzed to obtain highly accurate near-neighbor distances, coordination numbers and disorder parameters. Each atom at the same radial distance from the absorber contributes to the same component of the EXAFS signal. This group of atoms is called a shell. The number of atoms in the shell is called the coordination number. The oscillations corresponding to the different near-neighbor coordination shells can be described and modeled according to the EXAFS equation which is summed over all EXAFS absorber backscatterer pairs  $j$ :

$$\chi(k) = \sum_j \frac{N_j f_j(k) e^{-2k^2 \sigma_j}}{k R_j^2} \sin[2kR_j + \delta_j(k)] \quad (6)$$

where  $N$  is the number of neighboring atoms,  $f(k)$  and  $\delta(k)$  are the scattering properties of the atoms neighboring the excited atom (the amplitude and phase shift, respectively),  $R$  is the distance to the neighboring atom, and  $\sigma^2$  is the thermal disorder in the metal-neighbor distance (Debye-Waller factor). Analysis of the EXAFS equation for a given experimental spectra enables determining  $N$ ,  $R$  and  $\sigma^2$  with high accuracy providing high resolution structural information regarding the local environment around the excited metal ion.

## 2.2 Application of XAS in biology

Applying XAS to the study of biological systems has become widely used in the last three decades<sup>20-24</sup>. Since XAS accurately reports the structure of metal-protein centers, early workers focused on providing additional high resolution structural and electronic information on crystallographically characterized samples. For instance, XAS enabled detailed structural investigation of metal active sites in imidazolonepropionase<sup>25</sup>, cytochrome P450<sup>26, 27</sup>, CO dehydrogenase/acetyl-CoA synthase<sup>28-30</sup>, manganese catalases<sup>31, 32</sup>, and lipoxygenase<sup>33</sup> by providing key insights into their electronic states and atomic structures. Moreover, insights into the enzymatic reaction mechanisms could be derived from XAS analysis, as was shown for tyrosine hydroxylase<sup>34</sup>, molybdenum(Mo)-nitrogenase<sup>35-37</sup>, and farnesyltransferase<sup>38</sup>. Importantly, XAS is also a suitable method for characterizing metallodrug/protein interactions<sup>39</sup> and it was shown to be useful for resolving some of the apparent discrepancies among different spectroscopic and crystallographic studies of metalloproteins<sup>30</sup>. Also, XAS can provide structural information into metalloproteins that cannot be easily crystallized like membrane proteins.

## 2.3 Time-resolved XAS as a tool to investigate protein reaction mechanisms

One of the main advantages of XAS is that experiments can be carried in any state of the matter (e.g. solution and within membranes). This presents XAS as important tools to depict

structural transient changes during protein function. The first time-resolved X-ray absorption measurement was conducted at 1984 by Smith and coworkers following the reaction of recombination of carbon monoxide with myoglobin after laser photolysis with 300 μsec time resolution<sup>40</sup>. In laser photolysis (also known as 'pump-probe'), a particular bond of the reagent is cleaved by a pulse of light so that reactive intermediates are formed. EXAFS flash photolysis studies are performed by exciting the sample with a laser pulse and then exposing it to the X-ray beam for a rapid scan in order to characterize the evolving states upon excitation. Here, changes in the pre-edge structure and in the position of the iron edge of this protein as a function of time revealed several intermediates during binding of carbon monoxide to the iron metal center in myoglobin. Later experiments were used to characterize the photoproducts of Cob(II)alamin<sup>41</sup>, the nickel site of *chromatium vinosum* hydrogenase<sup>42</sup> and photosystem II<sup>43</sup>. However, the repertoire of biological reactions to which this approach can be applied is limited because a suitable target for the flash is rarely available.

Rapid freeze quenching<sup>44</sup> is a different strategy to capture transient reaction intermediates to be probed by a variety of spectroscopic methods such as time-resolved electron paramagnetic resonance (EPR) and solid-state nuclear magnetic resonance (NMR)<sup>45-49</sup>. The freeze-quench method is based on the coupling of rapid mixing of the reactants to a freezing device that quenches the reaction mixture in a given state and creates a stable sample. By repeating this process while allowing the reactants to react for various time periods before freezing, a series of different time-points along the reaction path are produced. The first application of the rapid freezing procedure to EXAFS studies was described by George et al. in their study of the molybdenum centre of xanthine oxidase<sup>50</sup>. This preliminary study provided the distances of the first shell coordinating atoms of a reaction intermediate formed after 600 msec, while it was known from other kinetic studies that at this time point the intermediate composed most of the reaction mixture. In later experiments, the feasibility of trapping single intermediate states during metalloenzyme catalysis by rapid freeze-quench was demonstrated for binuclear metalloenzyme systems<sup>51, 52</sup>. However, data analysis of multiple time-dependent samples requiring deconvolution of the data was not developed to this point.

Probing metalloenzyme reactions by time-dependent XAS procedures was suggested as a promising procedure to elucidate changes occurring in critical metal centers during the course of enzymatic reactions<sup>53, 54</sup>. Most challenging, however, is the correlation of structural and electronic changes in the metal ion's microenvironment with enzyme kinetics and protein structural dynamics. The principal difficulty in studying these critical questions is the inability to continuously follow the chemical and structural changes occurring at catalytic metal sites in real time. Inspired by this problem, we set out to advance the experimental approach of dynamic XAS on metalloenzymes during catalysis. Specifically, we introduced the use of quantitative structural-kinetic analyses of metalloenzymes in solution during their interactions with substrates and ligand. This experimental strategy employs stopped-flow freeze-quench XAS in conjunction with transient kinetic studies. By implementing the use of spectral convolution and non-linear curve fitting data analysis procedures, we could directly correlate structural and electronic changes as a function of distinct kinetic phases at atomic resolution<sup>55, 56</sup>. Owing to technical difficulties and the requirement of ample amounts of protein samples, the time-resolved XAS data collection remained challenging.

The following sections provide an overview on data collection and analyses using stopped-flow freeze-quench XAS and discuss the impact of this experimental strategy in revealing novel reaction mechanisms.

## 2.4 Stopped-flow XAS sample preparation and analysis procedures

### 2.4.1 Sample preparation

The experimental strategy utilizes stopped-flow freeze-quench XAS, which is conducted in conjunction with transient kinetic studies (Figure 4). To trap catalytic intermediates at the absorber metal ion during metalloenzyme catalysis, it is necessary to follow the off-equilibrium enzymatic rates. This allows following the formation of enzyme-substrate complexes prior to the steady-state reaction stage and improves the ability to trap and isolate evolving accumulated intermediate states resulting from their relatively high concentrations within this time frame. Transient reaction kinetics can be monitored by measuring the change in solution optical parameters, such as absorption or fluorescence, upon the formation of the reaction products, during the first catalytic cycles. Importantly, the reaction conditions of the transient kinetic experiments (concentration, buffer) should be equivalent to the conditions that will be later used during freeze-quench. Once the kinetic phases and time frame of the catalytic cycle are established, time points along the kinetic trace are selected for freeze-quench, usually 10-15 points along the different kinetic phases. In order to obtain a good XAS signal, the concentration of the metalloenzyme should be of at least hundreds of micromolars, to enable measuring the metal absorption spectra in fluorescence mode. Much higher concentrations should be used to measure the absorption in transmission mode. The samples for XAS are prepared in a stopped-flow instrument equipped with a freeze-quench device. Enzyme and substrate are mixed in the stopped-flow and freeze-quenched at selected time points into XAS sample holder by rapid freezing in a liquid nitrogen bath containing a freezing solution. These samples are kept frozen in special Dewars until taken to the synchrotron.

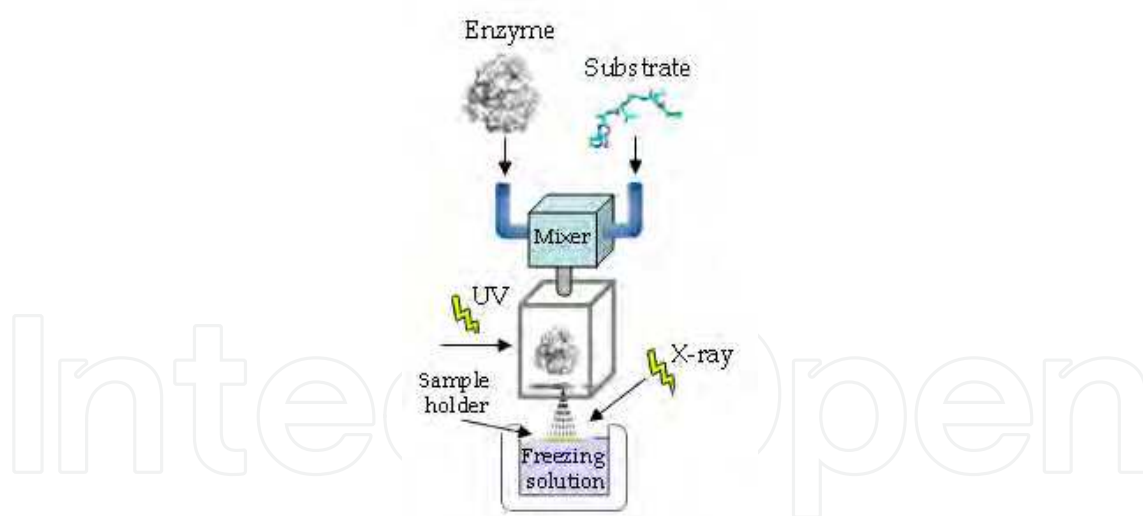


Fig. 4. Schematic representation of a stopped-flow XAS experimental setup to monitor kinetic phases involved in the proteolytic cycle of a metalloenzyme. This method allows one to establish a correlation between the pre-steady-state kinetic behavior of an enzyme and the structure of the evolving transient metal-protein intermediates as well as local charge transitions of the metal ion. The enzyme is rapidly mixed with substrate in a stopped-flow apparatus (mixing time = 2-5 ms). The instrument is equipped with a freeze-quench device. The pre-steady-state kinetic trace is monitored via an in-line fluorescence detector and analyzed. Enzyme/substrate mixtures are freeze-quenched at selected time point and mounted on an X-ray absorption sample holder.

### 2.4.2 Data analysis

EXAFS spectra of time-dependent measurements are particularly difficult to analyze since the spectra are composed of a disordered heterogeneous mixture of species, of which the mixing fractions change with time. Each species that contains the absorbing element may have a quite different local coordination around its nearest environment. This greatly complicates the non-linear curve fitting analysis used to extract the structural information, because the number of relevant structural parameters may be comparable to or may even exceed the number of independent data points in the experimental spectra. To account for this problem, we developed two complementary approaches for the EXAFS data analysis of mixtures, namely, **principal component analysis (PCA)** and **residual phase analysis (RPA)**<sup>57</sup>. Our data analysis strategy is shown in Figure 5.

PCA is initially used to estimate the number of minimal components required to convolute the EXAFS spectra. This procedure is sensitive to spectral changes that may be resolved by XAS. Using PCA, it is often possible to reveal (model-independently) the number of different species represented in the sample without a priori knowledge of their identity. However, these may not include all the reaction intermediates but instead only those that can be resolved by XAS. Each spectrum in the collection of EXAFS spectra measured at different time points may be represented by a linear combination of minimal components, which simplifies the data analysis procedure. The unique advantage of this method lies in its robustness and its model-independent determination of the number of unique species in the samples. If good experimental standards exist for representing each species, this method can also be reliably used to obtain both the identities and the mixing fractions of all the species in the sample<sup>58</sup>.

In order to obtain a crude assessment of structural intermediates with spectral signatures above the noise level, PCA is followed by **multiple data set fitting** analysis. This step provides general trends in the dynamic changes in coordination number and metal-ligand bond distances, while employing several chemically and physically reasonable constraints between the fitting parameters. Representative time points that exhibited the most pronounced spectral changes are simultaneously fit to a theoretical model. In this analysis, the variable fitting parameters corresponding to the atomic neighbors that are not estimated to undergo dramatic changes during turnover are constrained to be the same for all time points, while fitting parameters corresponding to atomic neighbors that undergo dynamic changes in the distance or coordination number remain varied. This way, the number of fit variables is reduced, enabling crude characterization of reaction intermediates without the need to fit the entire data.

The RPA approach utilizes one of the known components as a "starting phase". The "starting phase" is then fractionated and iteratively subtracted from the total XAS signal to produce the corresponding residual spectra. In a time-dependent experiment, the reaction zero point is usually selected to be the "starting phase" since the identity of this species is known in advance. This state is usually the free enzyme state (without substrate or ligand). Thus, the known phase EXAFS data are subtracted from the experimental data at each time step. The residual phase is analyzed with the fewer number of adjustable variables providing the best fit values. It also increases the confidence that relative differences in coordination numbers of the intermediates are real. The combination of PCA and RPA in time-resolved XAS analysis of metalloenzymes has been shown to simplify the data analysis procedure<sup>55,56</sup>.

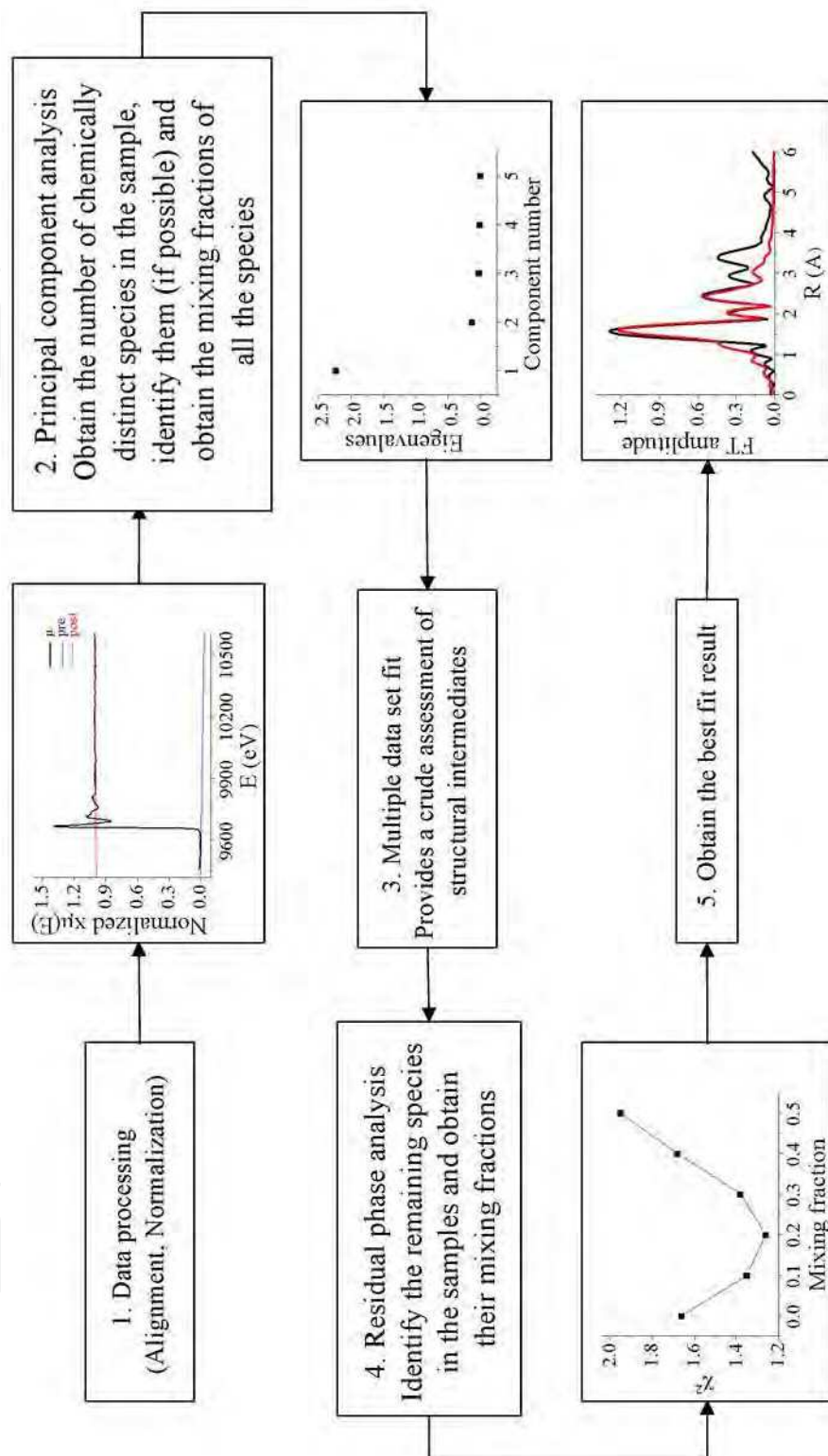


Fig. 5. **Time-resolved XAS data analysis strategy.** The processed data processing is analyzed by model-independent evaluation of the number of intermediate states by Principal Component Analysis (PCA), followed by a theoretical Multiple Data-Set (MDS) fit of the time-dependent data in order to identify possible models and, finally, the Residual Phase Analysis (RPA) study of the intermediate state, to obtain quantitative results.

Overall, these spectral analyses provide structural-kinetic models of XAS resolved reaction intermediates at a given reaction center. Importantly, the structure of the evolving intermediates and the total effective charge of the absorber ions may be directly correlated with the enzymatic kinetic trace. Thus, this experimental procedure provides the means to characterize metalloenzyme reaction pathways and hence to directly elucidate their molecular mechanisms under physiologically relevant solution conditions. Using stopped-flow XAS, we analyzed numerous bacterial and human zinc-dependent enzymes during the course of their enzymatic interactions<sup>55, 56, 59, 60</sup>. Remarkably, some of the derived mechanistic information was in striking contrast to the textbook mechanism in which the metal ion was proposed to remain attached to a fixed set of protein ligands. Probing the structural-kinetic reaction modes during metalloenzyme turnover indicated that there are dramatic differences in the nature of the metal ligation and the total effective charge of the catalytic metal ion. This further emphasizes the importance of dynamic fluctuations at the metal center in changing the electrostatic potential in the active site during the enzymatic reaction.

### 3. Mechanistic insights derived from stopped-flow/time-resolved XAS

#### 3.1 Stopped-Flow XAS provides novel insights into enzymatic mechanisms

A functional study of zinc in enzymology is in the focus of many fields owing to the important roles that this ion plays in biological systems<sup>61, 62</sup>. The flexibility in coordination geometry facilitates ligand exchange processes more than for other ions and enhances the ability of zinc to promote catalysis<sup>63</sup>. XAS is an excellent structural tool to probe the  $d^{10}$  zinc ion, which is generally spectroscopically silent. We therefore chose to begin our structural-kinetic studies on a bacterial member of the well-studied alcohol dehydrogenase (ADH) family, the zinc-dependent *Thermoanaerobacter brockii* alcohol dehydrogenase (TbADH).

This enzyme catalyzes the reversible oxidation of secondary alcohols to their corresponding ketones using  $NADP^+$  as the coenzyme<sup>64</sup>. Crystallographic studies of various alcohol dehydrogenases and their complexes indicate that this enzyme is a tetramer comprising four identical subunits. Each subunit contains a single catalytic zinc ion tetrahedrally coordinated by a single cysteine, histidine, aspartate, and glutamate residue<sup>11</sup>. The reaction mechanism has been investigated by spectroscopic and kinetic tools<sup>65</sup>; however the details of the ADH reaction mechanism remain controversial. Specifically, the intermediate states that evolve at the zinc ion during catalysis and the nature of its coordination chemistry have been the subject of debate for many years<sup>66-68</sup>. Two main types of structural mechanisms have been proposed for horse liver ADH (HLADH); they differ specifically in the hypothesized coordination of the zinc ion during catalysis. Dworschack and Plapp<sup>66</sup> proposed that the alcohol molecule is added to the tetrahedral zinc ion to form penta-coordinated zinc during catalysis. In contrast, Dunn *et al.*<sup>69</sup> proposed a mechanism whereby the substrate displaces the zinc-bound water without undergoing a penta-coordinated intermediate.

Applying stopped-flow freeze-quench XAS coupled with pre-steady-state kinetics to TbADH, it was possible to quantify the structure, electronics, and lifetimes of the evolving reaction intermediates at the catalytic zinc ion<sup>55</sup>. Specifically, pre-steady-state kinetic analysis revealed that the reaction consists of a lag period of 25 msec followed by a kinetic burst of 35 msec. Stopped-flow freeze-quenched raw X-ray fluorescence data detected a series of alternations in the coordination number and structure of the catalytic zinc ion with concomitant changes in metal-ligand bond distances. Even though stopped-flow XAS analysis cannot determine unambiguously the metal ion coordination numbers due to the

error associated with this measurement (which could be around  $\pm 1$ ), its advantage lies in the fact that each spectrum is compared relatively to the others. Non-linear curve fitting analysis of the Fourier transform (FT) of the EXAFS signal together with principal component analysis and residual phase analysis detected relative changes in the number of first shell neighbors along the reaction coordinates. Therefore, we were able to conclude that the zinc ion does not remain stationary during the reaction, but is undergoing changes in its coordination chemistry, as proposed by Dworschack et al.<sup>66</sup> and Makinen et al.<sup>70</sup> This study emphasizes the advantage of stopped-flow XAS in elucidating in real time the chemical nature of reaction intermediates that cannot be identified by any other means. Importantly, these results were recently supported by a series of high-resolution crystal structures of a relative enzyme, glucose dehydrogenase from *Haloflex mediterranei*, crystallized in the presence of substrates and products, in which dramatic differences in the nature of the zinc ligation were observed. Analysis of these structures revealed the direct consequence of linked movements of the zinc ion, a zinc-bound water molecule, and the substrate during progression through the reaction. In addition, it provided a structural explanation for multiple penta-coordinated zinc ion intermediates<sup>71</sup>.

The high-resolution structural-kinetic analyses of ADH raised the possibility that the dynamic nature of the catalytic zinc in this metalloenzyme is directly related to its function and thus it may be shared by other analogous systems. Accordingly, by applying stopped-flow XAS on human MMPs, we could directly correlate structural and electronics dynamics with function.

### **3.2 The functional effect of active site electronics and structural-kinetic transitions evolving during metalloproteinase action**

TNF $\alpha$ -converting enzyme (TACE) is the main shedding catalysis in the release of tumor necrosis factor- $\alpha$  (TNF $\alpha$ ) from its pro domain<sup>72</sup>. TACE is also critical for the release of a large number of cell surface proteins from the plasma membrane, including multiple cytokines and receptors<sup>73-75</sup>. TACE is a member of the *a* disintegrin and metalloproteinase (ADAM) family<sup>76</sup>. The ADAMs are highly homologous to the MMP family and are also characterized by the presence of a zinc metalloproteinase domain. The striking homology in 3D structures of the catalytic site of both families is the main obstacle in developing selective MMP and ADAM inhibitors.

Peptide hydrolysis by the MMP and the ADAM family members is facilitated via a nucleophilic attack of the zinc-bound water hydroxyl on the peptide scissile bond carbonyl. The structural and chemical knowledge underlying the enzymatic activity of these proteases is very limited. Most structural and biochemical studies, as well as medicinal chemistry efforts carried out so far, were limited to non-dynamic structure/function characterization. Substantial efforts have been aimed at better understanding the molecular basis by which the catalytic zinc machineries of metalloproteinases execute their enzymatic reactions. Protein crystallography, proteomic, and theoretical studies have been instrumental in proposing reaction mechanisms<sup>77-79</sup>. Structural snapshots of protein complexes with substrate analogues and inhibitors have suggested inconsistent and controversial reaction mechanisms. Applying stopped-flow XAS methodology to TACE provided the first structural-kinetic reaction model of a metalloproteinase in real time<sup>56</sup>. This allows one to visualize changes in a catalytic center that researchers have, until now, been unable to investigate. Remarkably, during the kinetic lag phase, dynamic charge transitions at the

active site zinc ion of TACE prior to substrate engagement with the ion were detected by time-dependent quantification of the change in edge energy at the zinc K-edge during peptide hydrolysis. This result implied communication between distal sites of the molecule and the catalytic core. The kinetic lag phase was followed by the binding of the peptide substrate to the zinc ion, forming a penta-coordinated transient complex, followed by product release and restoration of the tetrahedral zinc-protein complex. Thus, this work underscores the importance of local charge transitions critical for proteolysis as well as long-sought evidence for the proposed reaction model of peptide hydrolysis<sup>80</sup>. Furthermore, these results reveal novel communication pathways (yet unresolved) taking place between distal protein sites and the enzyme catalytic core (such as substrate-binding protein surfaces) and the catalytic machinery.

Interestingly, we have recently provided evidence that different MMPs and ADAMs possess variations in the polarity of the active site residues, which may be mediated by the specific enzyme/substrate surface interactions; these are reflected in typical electrostatic dynamics at the enzyme active site. Therefore, we hypothesize that these differences in active site electrostatics may be utilized in the rational design of selective inhibitors for this class of enzymes if their structural bases are also revealed<sup>81</sup>.

### 3.3 Probing active site structural-dynamics during catalytic protein-protein interactions

The advantage of having XAS measurement in solution during physiological interactions of macromolecules was extended to the analysis of structural-kinetic behavior of the catalytic zinc ion in MMPs during zymogen activation. Here we challenged the stopped flow freeze quench technology by exploring the feasibility of rapidly mixing two proteins, namely, pro-MMP-9 and the activator serine protease enzyme while we used dynamic XAS to directly probe the nearest environment of the catalytic zinc ion in pro-MMP-9 during the physiological activation process<sup>59</sup>.

The MMP family, as mentioned previously, comprises a large group of zinc-dependent endopeptidases involved in a variety of biological processes<sup>82</sup>. The MMPs are secreted or membrane tethered as zymogens as a control mechanism of MMP activity. The pro-peptide domain contains a "cysteine switch" PRCXXPD consensus sequence in which the cysteine coordinates to the zinc ion of the zymogen<sup>83</sup>. In this state, the catalytic zinc ion is tetrahedrally coordinated to three histidine residues and the conserved cysteine residue. Sequential proteolytic cleavages of the pro-domain by physiological proteases near the zinc-coordinated cysteine lead to replacement of the cysteine coordination shell by a water molecule and to the formation of an active enzyme. Activation of MMP zymogen is a vital homeostatic process; therefore, the structural and the kinetic bases of its molecular mechanism are of great interest<sup>84</sup>.

The kinetic time frame for full enzyme activation was determined using gel-based analysis<sup>85</sup> revealing that the MMP-9 pro-domain is cleaved at two points in two sequential proteolytic points mediated by tissue kallikrein. The initial cleavage (at 1 second) resulted in a relatively inactive intermediate in which the pro-domain remained bound to the enzyme shielding the catalytic zinc site from solution. Stopped-flow X-ray spectroscopy of the active site zinc ion was used to determine the temporal sequence of pro-MMP-9 zymogen activation catalyzed by tissue kallikrein protease. The identity of three intermediates seen by X-ray spectroscopy was corroborated by molecular dynamics simulations and QM/MM calculations.

Remarkably, the cysteine-zinc interaction that maintains enzyme latency is disrupted upon MMP-9-tissue kallikrein interactions at 400 milliseconds and the fourth ligand is replaced by a water molecule. QM/MM calculations indicated active site proton transfers that mediate three transient metal-protein coordination events prior to the binding of water. It was demonstrated that these events ensue as a direct result of complex formation between pro-MMP-9 and kallikrein, and occur prior to the pro-domain proteolysis and the eventual dissociation of the pro-peptide from the catalytic site. This work revealed that synergism exists among long-range protein conformational transitions, as well as local structural rearrangements, and that fine atomic events take place during the process of zymogen activation<sup>59</sup>. In addition, the proposed mechanisms provide the molecular basis for physiological non-proteolytic or allosteric activation mechanisms of MMPs by free radicals and macromolecular substrates.

#### **4. Integration of time-resolved XAS with structural-dynamic advanced experimental tools to probe functional protein conformational dynamics: Future prospects**

Proteins are flexible entities exhibiting backbone and side chain dynamics at various timescales that seems to play a crucial role in protein stability, function, and reactivity<sup>86</sup>. These protein motions were found to be critical for many biological events including enzyme catalysis, signal transduction, and protein-protein interactions<sup>87-89</sup>. Even though the three-dimensional structures of manifold functional proteins and enzymes are available, revealing molecular dynamic details that determine protein action and enzymatic functionality still represents a scientific challenge. Moreover, following these reactions in real time represents a major challenge in structural biology. Here, we have demonstrated the advantage of time-resolved XAS in characterizing the dynamic changes in the local atomic environment of metal active sites found in metalloenzymes during turnover with atomic resolution. However, this technique cannot provide broad molecular insights into functional structural-dynamic events taking place at other regions of the protein which are essential to its function. Moreover, stopped-flow XAS can only provide information on event taking place at the slow timescales (microseconds-milliseconds) due to the stopped-flow mixing times, neglecting information on events taking place at faster timescales. Thus, combining time-resolved XAS with complimentary hard core structural-dynamic experimental tools should provide a more comprehensive description of metalloenzymes during catalysis<sup>90</sup>.

A wealth of time-resolved structural-kinetic and spectroscopic techniques, including X-ray based techniques, have been developed in the last few decades to cope with these challenges, revealing the molecular structures of transient low-populated intermediate states<sup>90</sup>. Using time-resolved X-ray crystallography, it is possible to observe structural changes in crystals positioned in the X-ray beam by recording a time series of diffraction patterns using short X-ray pulses before and after the onset of a reaction<sup>91</sup>. By using sudden trigger events (e.g. laser-flash excitation) for initiating the reaction and by varying the delay time between the trigger and X-ray pulse, one can determine individual structures separated by time intervals of picoseconds<sup>92-94</sup>. Time-resolved wide-angle X-ray scattering (TR-WAXS) accurately probes tertiary and quaternary structural changes in proteins in solution with nanosecond time resolution<sup>95</sup>. In a TR-WAXS experiment, a laser pulse is used to trigger the protein's structural change, and transient structures are then

followed by delayed X-ray pulses from an undulator in a straight section of the synchrotron. Structural changes occurring in the sample leave their 'fingerprints' represented by the differences between the signals measured before and after the laser initiates the reaction; these differences can be monitored as a function of time<sup>96</sup>. Attempts to probe large conformational transitions of protein side chains by small angle X-ray scattering (SAXS) in real time currently are being developed by combining stopped-flow techniques and computational analysis. Similarly, introducing time-resolved Fourier transform infrared (FT-IR) spectroscopy to biochemistry enables one to investigate structural and functional properties of soluble and membrane proteins along their reaction pathways<sup>97-100</sup>. Here we outline only a few methods that provide a true means to follow protein conformational dynamics in real time as well as in equilibrium. Other methods such as mass spectroscopy (MS), NMR, and circular dichroism (CD) can also provide structural information during protein/nucleic acid functional dynamic events. Each of the described methods has the potential to yield key important mechanistic information. However, combining a few experimental tools that may probe different biophysical aspects of a given biological system can be more effective in deriving structure-based mechanistic information.

This concept is illustrated in our recent work in which we have developed an integrated experimental approach combining stopped-flow XAS together with kinetic terahertz absorption spectroscopy (KITA)<sup>101</sup>. KITA experiments were recently introduced for investigating solvation dynamics during biological reactions such as protein folding<sup>102</sup>. Our newly developed approach was used to study the correlation between structural-kinetic events taking place at an enzyme's active site with protein-water coupled motions during peptide hydrolysis by a MMP. Stopped-flow XAS in conjugation with transient kinetic analysis provided the structure and life time of evolving metal-protein reaction intermediates at the metalloenzyme active site. Integration of the KITA experiment under identical reaction conditions allowed quantification of collective protein-water motion during the various kinetic phases and in correlation to the evolved structural intermediates at the enzyme catalytic site. This highly integrated experimental approach provided novel insights into the proposed role of water motions in mediating enzyme catalysis. Specifically, it was demonstrated that a "slow to fast" gradient of water motions at the enzyme surface is gradually modified upon substrate binding at the enzyme active site. This study suggest that conformational fluctuations contributed by protein conformational transitions of both enzyme and substrates effect water motion kinetics. Such synergistic effect may assist enzyme-substrate interactions via remote water retardation effects and thus impact the enzymatic function.

## 5. Conclusions

Here we have described advancements in using time-dependent XAS to probe metalloenzymes during their physiological activities. Time-resolved XAS provides atomic resolution insights into the changes in the local structure and electronics of catalytic centers found in metalloenzymes during action. This information is often critical to reveal reaction mechanisms and structure-function relationships dictating the activity of this fascinating class of enzymes. This review also highlights the need to probe functional macromolecule conformational dynamics in order to obtain critical mechanistic information at atomic level detail. Better understanding of the dynamic characteristics of these metal centers may also

be crucial to drug design in structurally homologous enzymatic families. Future advancements may focus on overcoming the technical barriers encountered when combining real-time structural and spectroscopic experimental with X-ray absorption spectroscopy.

## 6. Acknowledgment

This work is supported by the Israel Science Foundation, the Kimmelman Center at the Weizmann Institute, and the Ambach family fund. I.S. is the incumbent of the Pontecorvo Professorial Chair.

## 7. References

- [1] W. Shi and M. R. Chance, *Current opinion in chemical biology*, 2011, 15, 144-148.
- [2] J. Finkelstein, *Nature*, 2009, 460, 813.
- [3] B. L. Vallee and D. S. Auld, *Matrix (Stuttgart, Germany)*, 1992, 1, 5-19.
- [4] D. S. Auld, *Biometals*, 2001, 14, 271-313.
- [5] C. R. Chong and D. S. Auld, *Biochemistry*, 2000, 39, 7580-7588.
- [6] C. E. Brinckerhoff and L. M. Matrisian, *Nature reviews*, 2002, 3, 207-214.
- [7] A. Page-McCaw, A. J. Ewald and Z. Werb, *Nature reviews*, 2007, 8, 221-233.
- [8] L. M. Matrisian, G. W. Sledge, Jr. and S. Mohla, *Cancer research*, 2003, 63, 6105-6109.
- [9] C. Lopez-Otin and L. M. Matrisian, *Nature reviews cancer*, 2007, 7, 800-808.
- [10] K. A. McCall, C. Huang and C. A. Fierke, *The Journal of nutrition*, 2000, 130, 1437S-1446S.
- [11] Y. Korkhin, A. J. Kalb, M. Peretz, O. Bogin, Y. Burstein and F. Frolow, *Journal of molecular biology*, 1998, 278, 967-981.
- [12] M. J. Ellis, F. E. Dodd, G. Sawers, R. R. Eady and S. S. Hasnain, *Journal of molecular biology*, 2003, 328, 429-438.
- [13] B. Govinda Rao, U. K. Bandarage, T. Wang, J. H. Come, E. Perola, Y. Wei, S. K. Tian and J. O. Saunders, *Bioorganic & medicinal chemistry letters*, 2007, 17, 2250-2253.
- [14] T. Arakawa, Y. Kawano, S. Kataoka, Y. Katayama, N. Kamiya, M. Yohda and M. Odaka, *Journal of molecular biology*, 2007, 366, 1497-1509.
- [15] V. V. Barynin, M. M. Whittaker, S. V. Antonyuk, V. S. Lamzin, P. M. Harrison, P. J. Artymiuk and J. W. Whittaker, *Structure*, 2001, 9, 725-738.
- [16] S. Y. Park, K. Yamane, S. Adachi, Y. Shiro, K. E. Weiss, S. A. Maves and S. G. Sligar, *Journal of inorganic biochemistry*, 2002, 91, 491-501.
- [17] K. Moffat, *Chemical reviews*, 2001, 101, 1569-1581.
- [18] B. L. Stoddard, *Methods*, 2001, 24, 125-138.
- [19] D. E. Sayers, E. A. Stern and F. W. Lytle, *Physical review letters*, 1971, 27, 1204-1207.
- [20] I. Ascone and R. Strange, *Journal of synchrotron radiation*, 2009, 16, 413-421.
- [21] L. Powers, J. L. Sessler, G. L. Woolery and B. Chance, *Biochemistry*, 1984, 23, 5519-5523.
- [22] E. Scheuring, S. Huang, R. G. Matthews and M. R. Chance, *Biophysical journal*, 1996, 70, Wp341-Wp341.
- [23] M. R. Chance, L. M. Miller, R. F. Fischetti, E. Scheuring, W. X. Huang, B. Sclavi, Y. Hai and M. Sullivan, *Biochemistry*, 1996, 35, 9014-9023.
- [24] S. K. Lee, S. D. George, W. E. Antholine, B. Hedman, K. O. Hodgson and E. I. Solomon, *Journal of the American Chemical Society*, 2002, 124, 6180-6193.

- [25] F. Yang, W. Chu, M. Yu, Y. Wang, S. Ma, Y. Dong and Z. Wu, *Journal of synchrotron radiation*, 2008, 15, 129-133.
- [26] M. Newcomb, J. A. Halgrimson, J. H. Horner, E. C. Wasinger, L. X. Chen and S. G. Sligar, *Proceedings of the National Academy of Sciences of the United States of America*, 2008, 105, 8179-8184.
- [27] A. Dey, Y. Jiang, P. Ortiz de Montellano, K. O. Hodgson, B. Hedman and E. I. Solomon, *Journal of the American Chemical Society*, 2009, 131, 7869-7878.
- [28] W. Gu, S. Gencic, S. P. Cramer and D. A. Grahame, *Journal of the American Chemical Society*, 2003, 125, 15343-15351.
- [29] J. Seravalli, W. Gu, A. Tam, E. Strauss, T. P. Begley, S. P. Cramer and S. W. Ragsdale, *Proceedings of the National Academy of Sciences of the United States of America*, 2003, 100, 3689-3694.
- [30] W. Gu, J. Seravalli, S. W. Ragsdale and S. P. Cramer, *Biochemistry*, 2004, 43, 9029-9035.
- [31] T. C. Weng, W. Y. Hsieh, E. S. Uffelman, S. W. Gordon-Wylie, T. J. Collins, V. L. Pecoraro and J. E. Penner-Hahn, *Journal of the American Chemical Society*, 2004, 126, 8070-8071.
- [32] A. J. Wu, J. E. Penner-Hahn and V. L. Pecoraro, *Chemical reviews*, 2004, 104, 903-938.
- [33] R. Sarangi, R. K. Hocking, M. L. Neidig, M. Benfatto, T. R. Holman, E. I. Solomon, K. O. Hodgson and B. Hedman, *Inorganic chemistry*, 2008, 47, 11543-11550.
- [34] M. S. Chow, B. E. Eser, S. A. Wilson, K. O. Hodgson, B. Hedman, P. F. Fitzpatrick and E. I. Solomon, *Journal of the American Chemical Society*, 2009, 131, 7685-7698.
- [35] C. C. Lee, M. A. Blank, A. W. Fay, J. M. Yoshizawa, Y. Hu, K. O. Hodgson, B. Hedman and M. W. Ribbe, *Proceedings of the National Academy of Sciences of the United States of America*, 2009, 106, 18474-18478.
- [36] Y. Hu, M. C. Corbett, A. W. Fay, J. A. Webber, K. O. Hodgson, B. Hedman and M. W. Ribbe, *Proceedings of the National Academy of Sciences of the United States of America*, 2006, 103, 17119-17124.
- [37] M. C. Corbett, Y. Hu, A. W. Fay, M. W. Ribbe, B. Hedman and K. O. Hodgson, *Proceedings of the National Academy of Sciences of the United States of America*, 2006, 103, 1238-1243.
- [38] D. A. Tobin, J. S. Pickett, H. L. Hartman, C. A. Fierke and J. E. Penner-Hahn, *Journal of the American Chemical Society*, 2003, 125, 9962-9969.
- [39] I. Ascone, L. Messori, A. Casini, C. Gabbiani, A. Balerna, F. Dell'Unto and A. C. Castellano, *Inorganic chemistry*, 2008, 47, 8629-8634.
- [40] D. M. Mills, A. Lewis, A. Harootunian, J. Huang and B. Smith, *Science*, 1984, 223, 811-813.
- [41] W. Clavin, E. Scheuring, M. Wirt, L. Miller, N. Mahoney, J. Wu, Y. Lu and M. R. Chance, *Biophysical journal*, 1994, 66, A378-A378.
- [42] G. Davidson, S. B. Choudhury, Z. Gu, K. Bose, W. Roseboom, S. P. Albracht and M. J. Maroney, *Biochemistry*, 2000, 39, 7468-7479.
- [43] M. Haumann, P. Liebisch, C. Muller, M. Barra, M. Grabolle and H. Dau, *Science*, 2005, 310, 1019-1021.
- [44] S. de Vries, *Freeze-Quench Kinetics*, John Wiley & Sons, Ltd, 2008.
- [45] R. J. Appleyard, W. A. Shuttleworth and J. N. Evans, *Biochemistry*, 1994, 33, 6812-6821.
- [46] M. Boll, G. Fuchs and D. J. Lowe, *Biochemistry*, 2001, 40, 7612-7620.

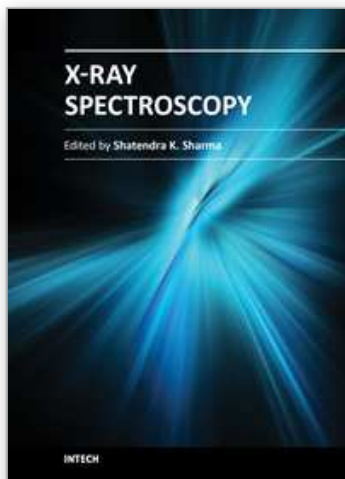
- [47] R. M. Jones, F. E. Inscore, R. Hille and M. L. Kirk, *Inorganic chemistry*, 1999, 38, 4963-4970.
- [48] L. Skipper, W. H. Campbell, J. A. Mertens and D. J. Lowe, *The Journal of biological chemistry*, 2001, 276, 26995-27002.
- [49] W. Zhang, K. K. Wong, R. S. Magliozzo and J. W. Kozarich, *Biochemistry*, 2001, 40, 4123-4130.
- [50] G. N. George, R. C. Bray and S. P. Cramer, *Biochemical society transactions*, 1986, 14, 651-652.
- [51] J. Hwang, C. Krebs, B. H. Huynh, D. E. Edmondson, E. C. Theil and J. E. Penner-Hahn, *Science*, 2000, 287, 122-125.
- [52] P. J. Riggs-Gelasco, L. Shu, S. Chen, D. Burdi, B. H. Huynh, J. P. Willems, L. Que and J. Stubbe, *Journal of the American Chemical Society*, 1998, 120, 849-860.
- [53] G. N. George, B. Hedman and K. O. Hodgson, *Nature structural biology*, 1998, 5 Suppl, 645-647.
- [54] M. A. Newton, A. J. Dent and J. Evans, *Chemical Society reviews*, 2002, 31, 83-95.
- [55] O. Kleifeld, A. Frenkel, J. M. Martin and I. Sagi, *Nature structural biology*, 2003, 10, 98-103.
- [56] A. Solomon, B. Akabayov, A. Frenkel, M. E. Milla and I. Sagi, *Proceedings of the National Academy of Sciences of the United States of America*, 2007, 104, 4931-4936.
- [57] A. I. Frenkel, O. Kleifeld, S. R. Wasserman and I. Sagi, *Journal of Chemical Physics*, 2002, 116, 9449-9456.
- [58] S. R. Wasserman, P. G. Allen, D. K. Shuh, J. J. Bucher and N. M. Edelstein, *Journal of synchrotron radiation*, 1999, 6, 284-286.
- [59] G. Rosenblum, S. Meroueh, M. Toth, J. F. Fisher, R. Fridman, S. Mobashery and I. Sagi, *Journal of the American Chemical Society*, 2007, 129, 13566-13574.
- [60] A. Solomon, G. Rosenblum, P. E. Gonzales, J. D. Leonard, S. Mobashery, M. E. Milla and I. Sagi, *The Journal of biological chemistry*, 2004, 279, 31646-31654.
- [61] D. Beyersmann and H. Haase, *Biometals*, 2001, 14, 331-341.
- [62] S. Frassinetti, G. Bronzetti, L. Caltavuturo, M. Cini and C. D. Croce, *Journal of environmental pathology, toxicology and oncology*, 2006, 25, 597-610.
- [63] G. Parkin, *Chemical Communications*, 2000, 1971-1985.
- [64] M. Peretz, O. Bogin, E. Keinan and Y. Burstein, *International journal of peptide and protein research*, 1993, 42, 490-495.
- [65] O. Kleifeld, A. Frenkel, O. Bogin, M. Eisenstein, V. Brumfeld, Y. Burstein and I. Sagi, *Biochemistry*, 2000, 39, 7702-7711.
- [66] R. T. Dworschack and B. V. Plapp, *Biochemistry*, 1977, 16, 111-116.
- [67] R. Meijers, R. J. Morris, H. W. Adolph, A. Merli, V. S. Lamzin and E. S. Cedergren-Zeppezauer, *The Journal of biological chemistry*, 2001, 276, 9316-9321.
- [68] L. Hemmingsen, R. Bauer, M. J. Bjerrum, M. Zeppezauer, H. W. Adolph, G. Formicka and E. Cedergren-Zeppezauer, *Biochemistry*, 1995, 34, 7145-7153.
- [69] M. F. Dunn, J. F. Biellmann and G. Branlant, *Biochemistry*, 1975, 14, 3176-3182.
- [70] M. W. Makinen, W. Maret and M. B. Yim, *Proceedings of the National Academy of Sciences of the United States of America*, 1983, 80, 2584-2588.
- [71] P. J. Baker, K. L. Britton, M. Fisher, J. Esclapez, C. Pire, M. J. Bonete, J. Ferrer and D. W. Rice, *Proceedings of the National Academy of Sciences of the United States of America*, 2009, 106, 779-784.

- [72] J. J. Peschon, J. L. Slack, P. Reddy, K. L. Stocking, S. W. Sunnarborg, D. C. Lee, W. E. Russell, B. J. Castner, R. S. Johnson, J. N. Fitzner, R. W. Boyce, N. Nelson, C. J. Kozlosky, M. F. Wolfson, C. T. Rauch, D. P. Cerretti, R. J. Paxton, C. J. March and R. A. Black, *Science*, 1998, 282, 1281-1284.
- [73] A. P. Huovila, A. J. Turner, M. Pelto-Huikko, I. Karkkainen and R. M. Ortiz, *Trends in biochemical sciences*, 2005, 30, 413-422.
- [74] C. P. Blobel, *Nature reviews*, 2005, 6, 32-43.
- [75] J. Arribas and A. Borroto, *Chemical reviews*, 2002, 102, 4627-4638.
- [76] T. G. Wolfsberg, P. Primakoff, D. G. Myles and J. M. White, *The Journal of cell biology*, 1995, 131, 275-278.
- [77] S. J. Benkovic and S. Hammes-Schiffer, *Science*, 2003, 301, 1196-1202.
- [78] I. Bertini, V. Calderone, M. Fragai, C. Luchinat, M. Maletta and K. J. Yeo, *Angewandte Chemie (International ed)*, 2006, 45, 7952-7955.
- [79] L. P. Kotra, J. B. Cross, Y. Shimura, R. Fridman, H. B. Schlegel and S. Mobashery, *Journal of the American Chemical Society*, 2001, 123, 3108-3113.
- [80] D. W. Christianson and W. N. Lipscomb, *Accounts Chem. Res.*, 1989, 22, 62-69.
- [81] I. Sagi and M. E. Milla, *Analytical biochemistry*, 2008, 372, 1-10.
- [82] K. Maskos and W. Bode, *Molecular biotechnology*, 2003, 25, 241-266.
- [83] E. B. Springman, E. L. Angleton, H. Birkedal-Hansen and H. E. Van Wart, *Proceedings of the National Academy of Sciences of the United States of America*, 1990, 87, 364-368.
- [84] H. J. Ra and W. C. Parks, *Matrix biology*, 2007, 26, 587-596.
- [85] P. D. Brown, A. T. Levy, I. M. Margulies, L. A. Liotta and W. G. Stetler-Stevenson, *Cancer research*, 1990, 50, 6184-6191.
- [86] K. Henzler-Wildman and D. Kern, *Nature*, 2007, 450, 964-972.
- [87] P. K. Agarwal, *Journal of the American Chemical Society*, 2005, 127, 15248-15256.
- [88] R. G. Smock and L. M. Gierasch, *Science*, 2009, 324, 198-203.
- [89] M. S. Marlow and A. J. Wand, *Biochemistry*, 2006, 45, 8732-8741.
- [90] M. Grossman, N. Sela-Passwell and I. Sagi, *Current opinion in structural biology*, 21, 678-85.
- [91] S. Westenhoff, E. Nazarenko, E. Malmerberg, J. Davidsson, G. Katona and R. Neutze, *Acta crystallographica*, 2010, 66, 207-219.
- [92] D. Bourgeois and A. Royant, *Current opinion in structural biology*, 2005, 15, 538-547.
- [93] V. Srajer, Z. Ren, T. Y. Teng, M. Schmidt, T. Ursby, D. Bourgeois, C. Pradervand, W. Schildkamp, M. Wulff and K. Moffat, *Biochemistry*, 2001, 40, 13802-13815.
- [94] F. Schotte, M. Lim, T. A. Jackson, A. V. Smirnov, J. Soman, J. S. Olson, G. N. Phillips, Jr., M. Wulff and P. A. Anfinrud, *Science*, 2003, 300, 1944-1947.
- [95] M. Andersson, E. Malmerberg, S. Westenhoff, G. Katona, M. Cammarata, A. B. Wohri, L. C. Johansson, F. Ewald, M. Eklund, M. Wulff, J. Davidsson and R. Neutze, *Structure*, 2009, 17, 1265-1275.
- [96] M. Cammarata, M. Levantino, F. Schotte, P. A. Anfinrud, F. Ewald, J. Choi, A. Cupane, M. Wulff and H. Ihee, *Nature methods*, 2008, 5, 881-886.
- [97] I. Radu, M. Schlegler, C. Bolwien and J. Heberle, *Photochemical and photobiological sciences*, 2009, 8, 1517-1528.
- [98] J. A. Wright and C. J. Pickett, *Chemical communications*, 2009, 5719-5721.
- [99] F. Garczarek and K. Gerwert, *Nature*, 2006, 439, 109-112.

- [100] F. Garczarek, J. Wang, M. A. El-Sayed and K. Gerwert, *Biophysical journal*, 2004, 87, 2676-2682.
- [101] M. Grossman, B. Born, M. Heyden, D. Tworowski, F. G. B., I. Sagi and M. Havenith, *Nature structural and molecular biology*, 2011, 18, 1102-1108.
- [102] S. J. Kim, B. Born, M. Havenith and M. Gruebele, *Angewandte Chemie (International ed)*, 2008, 47, 6486-6489.

IntechOpen

IntechOpen



## **X-Ray Spectroscopy**

Edited by Dr. Shatendra K Sharma

ISBN 978-953-307-967-7

Hard cover, 280 pages

**Publisher** InTech

**Published online** 01, February, 2012

**Published in print edition** February, 2012

The x-ray is the only invention that became a regular diagnostic tool in hospitals within a week of its first observation by Roentgen in 1895. Even today, x-rays are a great characterization tool at the hands of scientists working in almost every field, such as medicine, physics, material science, space science, chemistry, archeology, and metallurgy. With vast existing applications of x-rays, it is even more surprising that every day people are finding new applications of x-rays or refining the existing techniques. This book consists of selected chapters on the recent applications of x-ray spectroscopy that are of great interest to the scientists and engineers working in the fields of material science, physics, chemistry, astrophysics, astrochemistry, instrumentation, and techniques of x-ray based characterization. The chapters have been grouped into two major sections based upon the techniques and applications. The book covers some basic principles of satellite x-rays as characterization tools for chemical properties and the physics of detectors and x-ray spectrometer. The techniques like EDXRF, WDXRF, EPMA, satellites, micro-beam analysis, particle induced XRF, and matrix effects are discussed. The characterization of thin films and ceramic materials using x-rays is also covered.

### **How to reference**

In order to correctly reference this scholarly work, feel free to copy and paste the following:

Moran Grossman and Irit Sagi (2012). Application of Stopped-Flow and Time-Resolved X-Ray Absorption Spectroscopy to the Study of Metalloproteins Molecular Mechanisms, X-Ray Spectroscopy, Dr. Shatendra K Sharma (Ed.), ISBN: 978-953-307-967-7, InTech, Available from: <http://www.intechopen.com/books/x-ray-spectroscopy/application-of-stopped-flow-and-time-resolved-x-ray-absorption-spectroscopy-to-the-study-of-metallop>

**INTECH**  
open science | open minds

### **InTech Europe**

University Campus STeP Ri  
Slavka Krautzeka 83/A  
51000 Rijeka, Croatia  
Phone: +385 (51) 770 447  
Fax: +385 (51) 686 166  
[www.intechopen.com](http://www.intechopen.com)

### **InTech China**

Unit 405, Office Block, Hotel Equatorial Shanghai  
No.65, Yan An Road (West), Shanghai, 200040, China  
中国上海市延安西路65号上海国际贵都大饭店办公楼405单元  
Phone: +86-21-62489820  
Fax: +86-21-62489821

© 2012 The Author(s). Licensee IntechOpen. This is an open access article distributed under the terms of the [Creative Commons Attribution 3.0 License](#), which permits unrestricted use, distribution, and reproduction in any medium, provided the original work is properly cited.

IntechOpen

IntechOpen